Local Nucleation of Microtubule Bundles through Tubulin Concentration into a Condensed Tau Phase

HHS Public Access

Author manuscript

Cell Rep. Author manuscript; available in PMC 2018 February 28.

Published in final edited form as:

Cell Rep. 2017 September 05; 20(10): 2304–2312. doi:10.1016/j.celrep.2017.08.042.

Local Nucleation of Microtubule Bundles through Tubulin Concentration into a Condensed Tau Phase

Amayra Hernández-Vega[1], **Marcus Braun**[2,3], **Lara Scharrel**[1,2], **Marcus Jahnel**[1,4], **Susanne Wegmann**[5], **Bradley T. Hyman**[5], **Simon Alberti**[1], **Stefan Diez**[1,2,*], and **Anthony A. Hyman**[1,6,*]

[1]Max Planck Institute of Molecular Cell Biology and Genetics, Dresden 01307, Germany

[2]B CUBE–Center for Molecular Bioengineering, Technische Universität Dresden, Dresden 01307, Germany

[3]Institute of Biotechnology CAS, BIOCEV, Vestec 25250, Czech Republic

[4]BIOTEC, Biotechnology Center of the Technische Universität Dresden, Dresden 01307, Germany

[5]Department Neurology, Massachusetts General Hospital, Harvard Medical School, Charlestown, MA 02129, USA

SUMMARY

Non-centrosomal microtubule bundles play important roles in cellular organization and function. Although many diverse proteins are known that can bundle microtubules, biochemical mechanisms by which cells could locally control the nucleation and formation of microtubule bundles are understudied. Here, we demonstrate that the concentration of tubulin into a condensed, liquid-like compartment composed of the unstructured neuronal protein tau is sufficient to nucleate microtubule bundles. We show that, under conditions of macro-molecular crowding, tau forms liquid-like drops. Tubulin partitions into these drops, efficiently increasing tubulin concentration and driving the nucleation of microtubules. These growing microtubules form bundles, which deform the drops while remaining enclosed by diffusible tau molecules exhibiting a liquid-like behavior. Our data suggest that condensed compartments of microtubule bundling proteins could promote the local formation of microtubule bundles in neurons by acting as non-centrosomal microtubule nucleation centers and that liquid-like tau encapsulation could provide both stability and plasticity to long axonal microtubule bundles.

*Correspondence: stefan.diez@tu-dresden.de (S.D.), hyman@mpi-cbg.de (A.A.H.).
[6]Lead Contact

SUPPLEMENTAL INFORMATION

Supplemental Information includes Supplemental Experimental Procedures, seven figures, one table, ten movies, and one data file and can be found with this article online at http://dx.doi.org/10.1016/j.celrep.2017.08.042.

AUTHOR CONTRIBUTIONS

A.H.-V. and A.A.H. conceived the project. A.H.-V., M.B., S.D., and A.A.H. wrote the manuscript. M.B., L.S., and A.H.-V. performed the single-microtubule experiments and total internal reflection fluorescence (TIRF) microscopy images. M.B. also helped in designing experiments and project discussions. M.J. performed the optical tweezer experiments. A.H.-V. performed the rest of the experiments. S.W. helped with the experiments. S.A. and B.T.H. contributed to experimental design and data interpretation.

INTRODUCTION

In order to organize their microtubule arrays, neurons must solve a number of challenges. First, they must drive the nucleation of microtubules in a centrosome-independent manner. Second, they must organize microtubules into bundles, which can be millimeters long. Although there is considerable knowledge about how neurons use microtubule bundles for microtubule-based transport, we have less knowledge about how microtubule bundles form (Baas et al., 2005; Chen et al., 2017; Sanchez and Feldman, 2017; Tanaka and Kirschner, 1991). More generally, we have little information on how cells locally nucleate microtubules in a centrosome-independent manner (Matamoros and Baas, 2016; Sánchez-Huertas et al., 2016).

The local formation of microtubule asters has been well studied and is controlled by nucleation of microtubules at centrosomes. Here, it is thought that concentration of proteins at centrosomes can drive local nucleation of microtubule asters. Indeed, recent work suggests that tubulin concentration at centrosomes could be a key mechanism driving aster nucleation (Woodruff et al., 2017). However, the local nucleation of microtubule bundles is less studied, and we know little about the cell biology of this problem. What sorts of biochemical mechanisms could drive local nucleation and formation of microtubule bundles? Neurons are rich in unstructured microtubule-associated proteins (MAPs). An important component of the microtubule cytoskeleton in neurons is the protein tau. Tau, also known as MAPT (MAP tau), is found aggregated in a number of neurodegenerative disorders, including Alzheimer's disease, and has been genetically linked to some of these diseases (Arendt et al., 2016). In healthy brains, tau localizes to the axons of neurons, while other MAPs localize to dendrites (Aronov et al., 2001; Matus, 1988). In vitro, it can stimulate the growth rate of microtubules (Drechsel et al., 1992; Kadavath et al., 2015), as well as diffuse along and bundle microtubules (Chen et al., 1992; Chung et al., 2016; Hinrichs et al., 2012; Rosenberg et al., 2008).

Tau consists of up to four tubulin binding domains surrounded by intrinsically disordered regions (Figure 1A) (Mukrasch et al., 2009). Research suggests that many intrinsically disordered proteins can form liquid-like drops by demixing from buffer (Brangwynne et al., 2009; Elbaum-Garfinkle et al., 2015; Pak et al., 2016; Patel et al., 2015). Once these drops are formed, other client proteins can partition into the drops, where they are concentrated, with the degree of concentration depending on the partition coefficient. This concentration of client proteins provides a potential mechanism to increase the rates of reactions (Banjade and Rosen, 2014; Jiang et al., 2015; Li et al., 2012; Su et al., 2016).

Here, we demonstrate that under conditions of molecular crowding, tau forms liquid-like drops. Tubulin partitions into these drops, where it nucleates and drives the formation of microtubule bundles. These bundles deform the drops and remain enclosed by diffusible tau molecules, exhibiting a liquid-like behavior. We suggest that tau drops can drive the formation of microtubule bundles in neurons by acting as non-centrosomal microtubule nucleation centers and that a liquid-like encapsulation by tau could provide both stability and plasticity to long axonal microtubule bundles.

RESULTS

Many cytoskeleton regulatory proteins contain multiple binding sites for their polymer subunits and are, on average, highly disordered (Guharoy et al., 2013). Because both characteristics, multivalency and high intrinsic disorder, have been shown to be important traits for the formation of non-membrane-bound compartments (for review, see Banani et al., 2017), we wondered whether phase separation of cytoskeleton regulatory proteins could play a role in local control of cytoskeleton polymerization. As a starting point to address this question, we used the microtubule- associated protein tau. Tau is one of the first characterized intrinsically disordered proteins and contains up to four binding sites for tubulin (Figure 1A) (Mukrasch et al., 2009).

To investigate whether tau can form drops, we first expressed the protein in insect cells and purified it by affinity chromatography (Figure S1). A solution of tau is diffuse and forms no obvious structures. When we added a molecular crowder (10% dextran), tau phase-separated to form drops (Figure 1B). We confirmed the liquid-like nature of these drops by showing they (1) rapidly fused and relaxed into bigger drops (Figure 1C; Movie S1); (2) rapidly recovered their fluorescence after photo-bleaching, indicating that the protein in the drops is highly diffusible (Figure 1D; Movie S2); (3) wetted onto glass surfaces (Figure 1E; Movie S3); and (4) underwent fission (Figure 1E; Movie S3).

To further characterize the formation of tau drops and the possible contribution of molecular crowding, we investigated drop formation in different crowding agents and conditions. Tau drops were observed using dextran, PEG (polyethylene glycol), or Ficoll as the molecular crowder (Figure S2A). Drops were sensitive to the size and amount of the crowder, being enhanced by an increase in size or amount of the crowding agent (Figures S2B and S2C). Tau drops were also sensitive to the concentration of salt, being enhanced at low concentrations of salt and inhibited at high concentrations of salt (Figure S2D). The sensitivity to the ionic strength suggest that electrostatic interactions are important for the formation of tau drops and that drop formation could result from a complex coacervation effect, as suggested (Zhang et al., 2017).

To look at the interaction of tubulin with tau drops, we added tubulin (alpha/beta dimers) in the absence of guanosine triphosphate (GTP). Under these conditions, tubulin partitioned into drops (Figure 2A). The amount of tubulin partitioning into drops increased with increasing tubulin concentration (Figure S3A) such that the concentration inside the drop was consistently more than 10-fold higher than the concentration outside the drop (Figure 2B). As an example, when tubulin was added at an overall concentration of 1 μM, the concentration in the drop was higher than 20 μM (Figure S3B). The amount of tubulin partitioning into tau drops was similar when using HEPES buffer (pH 7.4) (Figures S3C and S3D). Tubulin stimulated the formation of tau drops, suggesting a positive feedback mechanism between tubulin partitioning and tau drop formation (Figures S4A and S4B). Because drop formation seems to be driven by electrostatic interaction and tau-tubulin interaction is also mediated by charge, we wondered whether RNA could also enhance the formation of tau drops (Saha et al., 2016). We found that under physiological conditions,

both tubulin and RNA facilitated the formation of tau drops in a similar way (Figures S4C and S4D) (Zhang et al., 2017).

To assess the potential role of tau drops as nucleators for the growth of microtubules, we repeated our experiment in the presence of GTP by adding 5 μM tubulin, together with 1 mM GTP, to preformed tau drops. The concentration of tubulin added was four times lower than the concentration needed for spontaneous nucleation of microtubules in vitro (Wieczorek et al., 2015). Within a few minutes of the addition of tubulin-GTP, tau drops deformed into rod-like shapes as microtubule bundles grew inside the drops (Figure 2C; Movies S4 and S5). Drop deformation was in most cases bidirectional (see Figure 2D for a typical example). At longer times, dense networks of tau-encapsulated microtubule bundles formed, and no individual drops remained (Figure 2E). Bundle formation in drops occurred under conditions in which the tubulin concentration in solution was as low as 0.75 μM (Figure 2F), more than an order of magnitude below the critical concentration for microtubule spontaneous nucleation in the absence of tau drops (Drechsel et al., 1992; Voter and Erickson, 1984; Wieczorek et al., 2015). In the absence of tau, regardless of the presence of crowding agents, 1–5 μM tubulin did not support microtubule nucleation or polymerization (Figure S5A) (Wieczorek et al., 2013, 2015).

To investigate whether the observed formation of microtubule bundles could be exclusively explained by a concentration effect, we analyzed microtubule polymerization using the concentrations of tubulin and tau estimated to be reached inside the drops but in the absence of drops (i.e., ≃ 175 μM of tubulin and 50 μM of tau in the absence of crowding agents). Mimicking tubulin and tau concentrations in the drops in a homogeneous environment generated many short microtubules surrounded by soluble tau but did not produce long bundled structures (rows 2 and 3 in Figure S5B). Likewise, no bundle formation was observed when mixing high concentrations of tubulin with 10% of the crowding agent. These data suggest that the bundles observed are due not solely to a concentration effect but rather to a combination of both concentration and confinement in the drops.

To further explore the nature of the tau-encapsulated microtubule bundles, we looked at the relative dynamics of tubulin and tau by photo-bleaching. When we photo-bleached the microtubule bundles, little recovery of the tubulin fluorescence was observed (Figure 3A; Movie S7). This supports the idea that the microtubules within the tau drops formed stable bundles. When we photo-bleached tau, it rapidly recovered (Figure 3A; Movie S7), demonstrating that tau molecules encapsulating the microtubules were freely diffusible. Tau thus exhibits a liquid-like behavior, which is underscored by the observation that tau-encapsulated microtubule bundles fused into larger assemblies (Figure 3B; Movie S8) and that tau drops without encapsulated microtubule bundles were able to fuse with pre-existing tau-encapsulated microtubule bundles (Figure 3C).

We next wondered what would happen when tubulin and GTP-loaded tau drops interacted with pre-existing microtubules. When we added tubulin and GTP-loaded tau drops to preassembled, stabilized microtubules, the drops bound to and directed the growth of new microtubules alongside the pre-existing microtubules (Figure 3D; Movie S9). These observations indicate that tau mediates attractive microtubule-microtubule interactions and

that tau drops alone or on top of pre-existing microtubules, efficiently polymerize microtubule bundles.

To examine the role of tau drops in stabilizing and bundling microtubules, we looked for conditions that would interfere with the interaction of tau and tubulin. For this purpose, we used heparin, a negatively charged polymer, which has been shown to interfere with the tau-tubulin interaction (Goedert et al., 1996). When we added heparin to tau-encapsulated microtubule bundles, tau lost its interaction with the microtubule bundles, reforming spherical drops (Figures 4A and 4B; Movie S10). At the same time, the naked microtubules unbundled (Figures 4A and 4B; Movie S10) and depolymerized (Figure S6). Presumably, tau drops facilitate the stabilization of microtubule bundles, by keeping the tubulin concentration in the surrounding compartment above the critical concentration and/or by stabilizing the microtubule lattice by its multiple binding sites.

DISCUSSION

Altogether, our experimental results show that tau can form liquid-like drops. Tubulin partitions into the drops, raising its local concentration above the critical concentration for nucleation of microtubules. These nucleated microtubules form bundles and, while growing, collectively deform the tau drops into rod-like shapes of a tau-encapsulated, microtubule-bundled structure (see the model in Figure 4C). Tau's multiple binding sites for tubulin, binding with low affinity at the interface between tubulin hetero-dimers, together with its conformational flexibility and its capability to interact with itself, are likely contributing to the liquid-like behavior of the tau encapsulation, the nucleation of new microtubules, and the formation of microtubule bundles (Igaev et al., 2014; Janning et al., 2014; Kadavath et al., 2015; Li et al., 2015; Li and Rhoades, 2017; Melo et al., 2016).

We found that the high concentrations alone of tau and tubulin reached in the drops are not sufficient to generate microtubule bundles in a homogeneous environment, suggesting that the environment of the drop is important for the observed phenomena. We can only speculate what aspect of the drops does drive the bundling, but constrained diffusion of the nucleated microtubules inside the drop may play a crucial role.

We do not know whether similar mechanisms operate in vivo. Tau is known to localize to microtubule bundles in vivo, suggesting a role in organizing microtubule bundles. Although the mouse knockout of tau shows little phenotype, the double-knockout Tau/MAP1b has severe phenotypes (Takei et al., 2000; Tortosa et al., 2016) and the deletion of tau results in upregulation of another MAP, MAP2, suggesting a compensatory mechanism (Ma et al., 2014). A manuscript under review looking at the expression of GFP-tau constructs in neurons suggests that they also form higher-order assemblies in vivo (S.W., B. Eftekharzadeh, K. Tepper, K.M. Zoltowska, R.E. Bennett, A.M. Molliex, S. Dujardin, D. MacKenzie, C. Commins, Z. Fan, P.R. Laskowski, A.H.-V., D. Muller, J.P. Taylor, A.A.H., E. Mandelkow, B.T.H., unpublished data). Our experiments require molecular crowders to drive the formation of tau drops at physiological salt concentrations. Presumably, this is substituting for a tau drop nucleating factor that exists in vivo. Our results suggest that tubulin itself—and maybe RNA—is part of the nucleation mechanism. The formation of tau

drops has been reported to occur in the absence of molecular crowders using RNA as nucleator under conditions of low salt and low pH; a tau-tRNA association in vivo was also observed in this study (Zhang et al., 2017).

We hypothesize that in polarizing neurons, tau mRNA could be locally stabilized, producing tau protein at one side of the cell (Aronov et al., 2001; Dickson et al., 2013; Malmqvist et al., 2014). Polarity-mediated phosphorylation could be an alternative mechanism to regulate the local formation of tau drops in the future axon (Herzmann et al., 2017; Zempel and Mandelkow, 2014). Tau drops will recruit tubulin and polymerize microtubule bundles alone or on top of pre-existing microtubules, enabling the formation of axonal microtubule bundles. A feedback loop mechanism mediated by tubulin or an enhancement of tau drops by RNA (Malmqvist et al., 2014; Zhang et al., 2017) would be also plausible. More work on the formation of microtubule bundles in axons will be required to distinguish among these possibilities.

Although our work has focused on tau, our experiments suggest that phase separation of cytoskeleton regulatory proteins in general could be an efficient way of locally controlling cytoskeleton polymerization and bundling. Other closely related MAPs (MAP2 and MAP4) display a charge distribution similar to that of tau, suggesting a possibly conserved mechanism (Figure S7A). A brush model has been proposed for both tau and neurofilaments (Kornreich et al., 2015; Mukhopadhyay et al., 2004). Although the charge distribution of different intermediate filaments is different from that of tau, most have a conserved, positively charged region in its head domain (Figure S7C). This part of the protein has been shown to be essential for its bundling capability (reviewed in Herrmann and Aebi, 2004).

Work on other unstructured proteins such as FUS has suggested that a liquid-solid phase transition is involved in the onset of protein aggregation in the motor neuron disease amyotrophic lateral sclerosis (ALS) (Patel et al., 2015). Tau can also form liquid-like drops, suggesting that such liquid-solid phase transitions could be involved in the onset of Alzheimer's disease (S.W., B. Eftekharzadeh, K. Tepper, K.M. Zoltowska, R.E. Bennett, A.M. Molliex, S. Dujardin, D. MacKenzie, C. Commins, Z. Fan, P.R. Laskowski, A.H.-V., D. Muller, J.P. Taylor, A.A.H., E. Mandelkow, B.T.H., unpublished data). We have developed an easy in vitro system to check for this transition and the relation between tau function in microtubules and its aggregation state. We hope that competition experiments with tau mutations implicated in neurodegenerative diseases will help us understanding better the cause of these diseases in the future.

Our work supports the idea that the local concentration of tubulin, driven by phase separation of regulatory factors, could be a general mechanism driving the formation of microtubule arrays. Concentration of tubulin has been proposed to be a mechanism driving nucleation of microtubules in C. elegans centrosomes (Woodruff et al., 2017). In Xenopus extracts, the protein BuGZ has been shown to form liquid-like drops into which tubulin can partition and polymerize microtubules, suggesting a mechanism for spindle formation (Jiang et al., 2015). A similar mechanism for promoting local actin polymerization by its recruitment into phase-separated compartments was also observed (Banjade and Rosen, 2014; Li et al., 2012; Su et al., 2016). These experiments, together with our findings, suggest

that the concentration of cytoskeletal monomers into liquid-like drops of cytoskeletal regulatory proteins could be a general mechanism for the formation of local nucleation centers for cytoskeletal filaments. The types of arrays that arise from this concentration mechanism, whether bundles or asters, would depend on the type of MAPs present in the drops.

EXPERIMENTAL PROCEDURES

Constructs Used and Protein Purification

A human tau isoform with 4 putative binding sites for tubulin (htau441, also named 2N4R) was used for all experiments. Recombinant htau441-6xhis, htau441-EGFP-6xhis, and htau441-mCherry-6xhis were purified from insect cells using a his tag. The tag was cleaved at the end of the purification. For more info, see Supplemental Experimental Procedures. Porcine tubulin was used throughout the study. Tubulin was purified as previously described (Gell et al., 2011).

Drop Formation

25 μM of tau-EGFP was used for drop formation in this study, if not otherwise mentioned. To form the drops, 36 to 50 μM tau-EGFP in 25 mM HEPES and 150 mM KCl (pH 7.4) with freshly added DTT (1 mM) was mixed with 20% dextran (Dextran T500, Cat. No. 40030, Pharmacosmos) 1:1 to a final concentration of 18 to 25 μM tau-EGFP and 10% dextran. 18 μM of tau-EGFP was the lowest concentration at which we observed drop formation at 10% dextran without another nucleation factor. T500 dextran was used as the molecular crowder throughout this study, if not otherwise mentioned. Different sizes of PEG, ranging from 600 to 35,000 Da (Sigma), were also used at the concentration indicated in each figure. Drops were also formed with 10% Ficoll-400 (Sigma) where indicated. In all experiments with tubulin, 13 BRB80 (80 mM PIPES, 1 mM EGTA, 1 mM $MgCl_2$ [pH 6.9]) was used to dilute the protein and the dextran, if not otherwise mentioned. For further assays of drops' liquid-like behavior, see Supplemental Experimental Procedures.

Microtubule Bundle Formation

Porcine tubulin dimers (unlabeled or rhodamine labeled) were added to tau drops at a 5 μM concentration, together with 1 mM GTP, if not otherwise mentioned. Tau drops were formed with 25 μM tau-EGFP and 10% dextran in 13 BRB80 with 1 mM DTT. Drop deformation and microtubule bundle polymerization equally occurred in 25 mM HEPES and 150 mM KCl (pH 7.4) when tubulin and GTP were added. All experiments were carried out at room temperature.

Heparin Treatment

Heparin sodium salt from porcine intestinal mucosa (Cat. No. H3393, Sigma) was added to tau-encapsulated microtubule bundles at a final concentration of 200 μg/mL.

Quantification and Statistical Analysis

Images were analyzed using Fiji (Schindelin et al., 2012). For the experiments calculating tubulin and tau enrichment in tau drops and tau drop nucleation by tubulin or RNA, image z stacks (50 images per stack) were segmented using an intensity threshold. The threshold was calculated using the following formula: $T = I_0 + A * SD$. The A parameter was set to a value of 11 for all images based on empirical results for best drop segmentation in a z stack. A segmentation mask was generated using the tau intensity signal, and the mask was applied for both tau and tubulin measurements. The average intensities for each protein and the ratio of the average intensity inside to the average intensity outside the drops was calculated. For the nucleation experiments, the normalized sum intensity of all drops in the z stack was used. The camera background was subtracted for each channel in all measurements. All data are expressed as the mean ± SD. The mean and SD of 16 z stacks with 50 images each stack was calculated for all measurements. 50 images were analyzed for each z stack. All experiments were repeated 3 times, and the average and SD of the 3 biological replicas is calculated where stated. The script used for the analysis of the drops can be found in Data S1.

FRAP Analysis

The FRAP Calculator macro generated by Robert Bagnell was used to analyze the bleached regions (https://www.med.unc.edu/microscopy/resources/imagej-plugins-and-macros/frap-calculator-macro). The plugin corrects the data for photo-bleaching due to the imaging process. Values were normalized to the intensity before photo-bleaching.

Supplementary Material

Refer to Web version on PubMed Central for supplementary material.

Acknowledgments

We thank David Drechsel, Jan Brugués, Gaia Pigino, Titus Franzmann, Avinash Patel, and Mark Leaver for comments and discussions on earlier versions of this manuscript. We thank the Protein Expression and Purification facility at Max Planck Institute of Molecular Cell Biology and Genetics (MPI-CBG; Dresden), especially David Drechsel, Barbara Borgonovo, Régis Lemaitre, and Martine Ruer, for help with protein purification. The Light Microscopy facility at MPI-CBG (Dresden) helped with image acquisition. Benoit Lombardot from the Scientific Computing Facility at the MPI-CBG (Dresden) developed the script to segment and analyze drop numbers and partition coefficients. Andrei Pozniakovsky and Aliona Bogdanova helped with cloning DNA constructs. Avinash Patel, Titus Franzmann, Shamba Saha, Jie Wang, Mark Leaver, and other members of Hyman, Diez, and Alberti laboratories gave suggestions and help with in vitro experiments. This project was funded by the Bundesministerium für Bildung und Forschung (PDdementia, 01EK1606C) and the Max Planck Society.

References

Arendt T, Stieler JT, Holzer M. Tau and tauopathies. Brain Res. Bull. 2016; 126:238–292. [PubMed: 27615390]

Aronov S, Aranda G, Behar L, Ginzburg I. Axonal tau mRNA localization coincides with tau protein in living neuronal cells and depends on axonal targeting signal. J. Neurosci. 2001; 21:6577–6587. [PubMed: 11517247]

Baas PW, Karabay A, Qiang L. Microtubules cut and run. Trends Cell Biol. 2005; 15:518–524. [PubMed: 16126385]

Banani SF, Lee HO, Hyman AA, Rosen MK. Biomolecular condensates: organizers of cellular biochemistry. Nat. Rev. Mol. Cell Biol. 2017; 18:285–298. [PubMed: 28225081]

Banjade S, Rosen MK. Phase transitions of multivalent proteins can promote clustering of membrane receptors. eLife. 2014; 3:e04123.

Brangwynne CP, Eckmann CR, Courson DS, Rybarska A, Hoege C, Gharakhani J, Jülicher F, Hyman AA. Germline P granules are liquid droplets that localize by controlled dissolution/condensation. Science. 2009; 324:1729–1732. [PubMed: 19460965]

Chen J, Kanai Y, Cowan NJ, Hirokawa N. Projection domains of MAP2 and tau determine spacings between microtubules in dendrites and axons. Nature. 1992; 360:674–677. [PubMed: 1465130]

Chen W-S, Chen Y-J, Huang Y-A, Hsieh B-Y, Chiu H-C, Kao P-Y, Chao C-Y, Hwang E. Ran-dependent TPX2 activation promotes acentrosomal microtubule nucleation in neurons. Sci. Rep. 2017; 7:42297. [PubMed: 28205572]

Chung PJ, Song C, Deek J, Miller HP, Li Y, Choi MC, Wilson L, Feinstein SC, Safinya CR. Tau mediates microtubule bundle architectures mimicking fascicles of microtubules found in the axon initial segment. Nat. Commun. 2016; 7:12278. [PubMed: 27452526]

Dickson JR, Kruse C, Montagna DR, Finsen B, Wolfe MS. Alternative polyadenylation and miR-34 family members regulate tau expression. J. Neurochem. 2013; 127:739–749. [PubMed: 24032460]

Drechsel DN, Hyman AA, Cobb MH, Kirschner MW. Modulation of the dynamic instability of tubulin assembly by the microtubule-associated protein tau. Mol. Biol. Cell. 1992; 3:1141–1154. [PubMed: 1421571]

Elbaum-Garfinkle S, Kim Y, Szczepaniak K, Chen CC-H, Eckmann CR, Myong S, Brangwynne CP. The disordered P granule protein LAF-1 drives phase separation into droplets with tunable viscosity and dynamics. Proc. Natl. Acad. Sci. USA. 2015; 112:7189–7194. [PubMed: 26015579]

Gell C, Friel CT, Borgonovo B, Drechsel DN, Hyman AA, Howard J. Purification of tubulin from porcine brain. Methods Mol. Biol. 2011; 777:15–28. [PubMed: 21773918]

Goedert M, Jakes R, Spillantini MG, Hasegawa M, Smith MJ, Crowther RA. Assembly of microtubule-associated protein tau into Alzheimer-like filaments induced by sulphated glycosaminoglycans. Nature. 1996; 383:550–553. [PubMed: 8849730]

Guharoy M, Szabo B, Contreras Martos S, Kosol S, Tompa P. Intrinsic structural disorder in cytoskeletal proteins. Cytoskeleton. 2013; 70:550–571. [PubMed: 23761374]

Herrmann H, Aebi U. Intermediate filaments: molecular structure, assembly mechanism, and integration into functionally distinct intracellular Scaffolds. Annu. Rev. Biochem. 2004; 73:749–789. [PubMed: 15189158]

Herzmann S, Krumkamp R, Rode S, Kintrup C, Rumpf S. PAR-1 promotes microtubule breakdown during dendrite pruning in Drosophila. EMBO. J. 2017; 36:1981–1991. [PubMed: 28554895]

Hinrichs MH, Jalal A, Brenner B, Mandelkow E, Kumar S, Scholz T. Tau protein diffuses along the microtubule lattice. J. Biol. Chem. 2012; 287:38559–38568. [PubMed: 23019339]

Igaev M, Janning D, Sündermann F, Niewidok B, Brandt R, Junge W. A refined reaction-diffusion model of tau-microtubule dynamics and its application in FDAP analysis. Biophys. J. 2014; 107:2567–2578. [PubMed: 25468336]

Janning D, Igaev M, Sündermann F, Brühmann J, Beutel O, Heinisch JJ, Bakota L, Piehler J, Junge W, Brandt R. Single-molecule tracking of tau reveals fast kiss-and-hop interaction with microtubules in living neurons. Mol. Biol. Cell. 2014; 25:3541–3551. [PubMed: 25165145]

Jiang H, Wang S, Huang Y, He X, Cui H, Zhu X, Zheng Y. Phase transition of spindle-associated protein regulate spindle apparatus assembly. Cell. 2015; 163:108–122. [PubMed: 26388440]

Kadavath H, Hofele RV, Biernat J, Kumar S, Tepper K, Urlaub H, Mandelkow E, Zweckstetter M. Tau stabilizes microtubules by binding at the interface between tubulin heterodimers. Proc. Natl. Acad. Sci. USA. 2015; 112:7501–7506. [PubMed: 26034266]

Kornreich M, Avinery R, Malka-Gibor E, Laser-Azogui A, Beck R. Order and disorder in intermediate filament proteins. FEBS Lett. 2015; 589(19 Pt A):2464–2476. [PubMed: 26231765]

Li X-H, Rhoades E. Heterogeneous tau-tubulin complexes accelerate microtubule polymerization. Biophys. J. 2017; 112:2567–2574. [PubMed: 28636913]

Li P, Banjade S, Cheng HC, Kim S, Chen B, Guo L, Llaguno M, Hollingsworth JV, King DS, Banani SF, et al. Phase transitions in the assembly of multivalent signalling proteins. Nature. 2012; 483:336–340. [PubMed: 22398450]

Li X-H, Culver JA, Rhoades E. Tau binds to multiple tubulin dimers with helical structure. J. Am. Chem. Soc. 2015; 137:9218–9221. [PubMed: 26165802]

Ma Q-L, Zuo X, Yang F, Ubeda OJ, Gant DJ, Alaverdyan M, Kiosea NC, Nazari S, Chen PP, Nothias F, et al. Loss of MAP function leads to hippocampal synapse loss and deficits in the Morris water maze with aging. J. Neurosci. 2014; 34:7124–7136. [PubMed: 24849348]

Malmqvist T, Anthony K, Gallo J-M. Tau mRNA is present in axonal RNA granules and is associated with elongation factor 1A. Brain Res. 2014; 1584:22–27. [PubMed: 24389033]

Matamoros AJ, Baas PW. Microtubules in health and degenerative disease of the nervous system. Brain Res. Bull. 2016; 126:217–225. [PubMed: 27365230]

Matus A. Microtubule-associated proteins: their potential role in determining neuronal morphology. Annu. Rev. Neurosci. 1988; 11:29–44. [PubMed: 3284444]

Melo AM, Coraor J, Alpha-Cobb G, Elbaum-Garfinkle S, Nath A, Rhoades E. A functional role for intrinsic disorder in the tau-tubulin complex. Proc. Natl. Acad. Sci. USA. 2016; 113:14336–14341. [PubMed: 27911791]

Mukhopadhyay R, Kumar S, Hoh JH. Molecular mechanisms for organizing the neuronal cytoskeleton. BioEssays. 2004; 26:1017–1025. [PubMed: 15351972]

Mukrasch MD, Bibow S, Korukottu J, Jeganathan S, Biernat J, Griesinger C, Mandelkow E, Zweckstetter M. Structural polymorphism of 441-residue tau at single residue resolution. PLoS Biol. 2009; 7:e34. [PubMed: 19226187]

Pak CW, Kosno M, Holehouse AS, Padrick SB, Mittal A, Ali R, Yunus AA, Liu DR, Pappu RV, Rosen MK. Sequence determinants of intracellular phase separation by complex coacervation of a disordered protein. Mol. Cell. 2016; 63:72–85. [PubMed: 27392146]

Patel A, Lee HO, Jawerth L, Maharana S, Jahnel M, Hein MY, Stoynov S, Mahamid J, Saha S, Franzmann TM, et al. A liquid-to-solid phase transition of the ALS protein FUS accelerated by disease mutation. Cell. 2015; 162:1066–1077. [PubMed: 26317470]

Rosenberg KJ, Ross JL, Feinstein HE, Feinstein SC, Israelachvili J. Complementary dimerization of microtubule-associated tau protein: implications for microtubule bundling and tau-mediated pathogenesis. Proc. Natl. Acad. Sci. USA. 2008; 105:7445–7450. [PubMed: 18495933]

Saha S, Weber CA, Nousch M, Adame-Arana O, Hoege C, Hein MY, Osborne-Nishimura E, Mahamid J, Jahnel M, Jawerth L, et al. Polar positioning of phase-separated liquid compartments in cells regulated by an mRNA competition mechanism. Cell. 2016; 166:1572–1584. [PubMed: 27594427]

Sanchez AD, Feldman JL. Microtubule-organizing centers: from the centrosome to non-centrosomal sites. Curr. Opin. Cell Biol. 2017; 44:93–101. [PubMed: 27666167]

Sánchez-Huertas C, Freixo F, Viais R, Lacasa C, Soriano E, Lüders J. Non-centrosomal nucleation mediated by augmin organizes micro-tubules in post-mitotic neurons and controls axonal microtubule polarity. Nat. Commun. 2016; 7:12187. [PubMed: 27405868]

Schindelin J, Arganda-Carreras I, Frise E, Kaynig V, Longair M, Pietzsch T, Preibisch S, Rueden C, Saalfeld S, Schmid B, et al. Fiji: an open-source platform for biological-image analysis. Nat. Methods. 2012; 9:676–682. [PubMed: 22743772]

Su X, Ditlev JA, Hui E, Xing W, Banjade S, Okrut J, King DS, Taunton J, Rosen MK, Vale RD. Phase separation of signaling molecules promotes T cell receptor signal transduction. Science. 2016; 352:595–599. [PubMed: 27056844]

Takei Y, Teng J, Harada A, Hirokawa N. Defects in axonal elongation and neuronal migration in mice with disrupted tau and map1b genes. J. Cell Biol. 2000; 150:989–1000. [PubMed: 10973990]

Tanaka EM, Kirschner MW. Microtubule behavior in the growth cones of living neurons during axon elongation. J. Cell Biol. 1991; 115:345–363. [PubMed: 1918145]

Tortosa, E., Kapitein, LC., Hoogenraad, CC. Microtubule organization and microtubule-associated proteins (MAPs). In: Emoto, K.Wong, R.Huang, E., Hoogenraad, C., editors. Dendrites. Springer; 2016. p. 31-75.

Voter WA, Erickson HP. The kinetics of microtubule assembly. Evidence for a two-stage nucleation mechanism. J. Biol. Chem. 1984; 259:10430–10438. [PubMed: 6469971]

Wieczorek M, Chaaban S, Brouhard GJ. Macromolecular crowding pushes catalyzed microtubule growth to near the theoretical limit. Cell. Mol. Bioeng. 2013; 6:383–392.

Wieczorek M, Bechstedt S, Chaaban S, Brouhard GJ. Microtubule- associated proteins control the kinetics of microtubule nucleation. Nat. Cell Biol. 2015; 17:907–916. [PubMed: 26098575]

Woodruff JB, Ferreira Gomes B, Widlund PO, Mahamid J, Honigmann A, Hyman AA. The centrosome is a selective condensate that nucleates microtubules by concentrating tubulin. Cell. 2017; 169:1066–1077. [PubMed: 28575670]

Zempel H, Mandelkow E. Lost after translation: missorting of Tau protein and consequences for Alzheimer disease. Trends Neurosci. 2014; 37:721–732. [PubMed: 25223701]

Zhang X, Lin Y, Eschmann NA, Zhou H, Rauch JN, Hernandez I, Guzman E, Kosik KS, Han S. RNA stores tau reversibly in complex coacervates. PLoS Biol. 2017; 15:e2002183. [PubMed: 28683104]

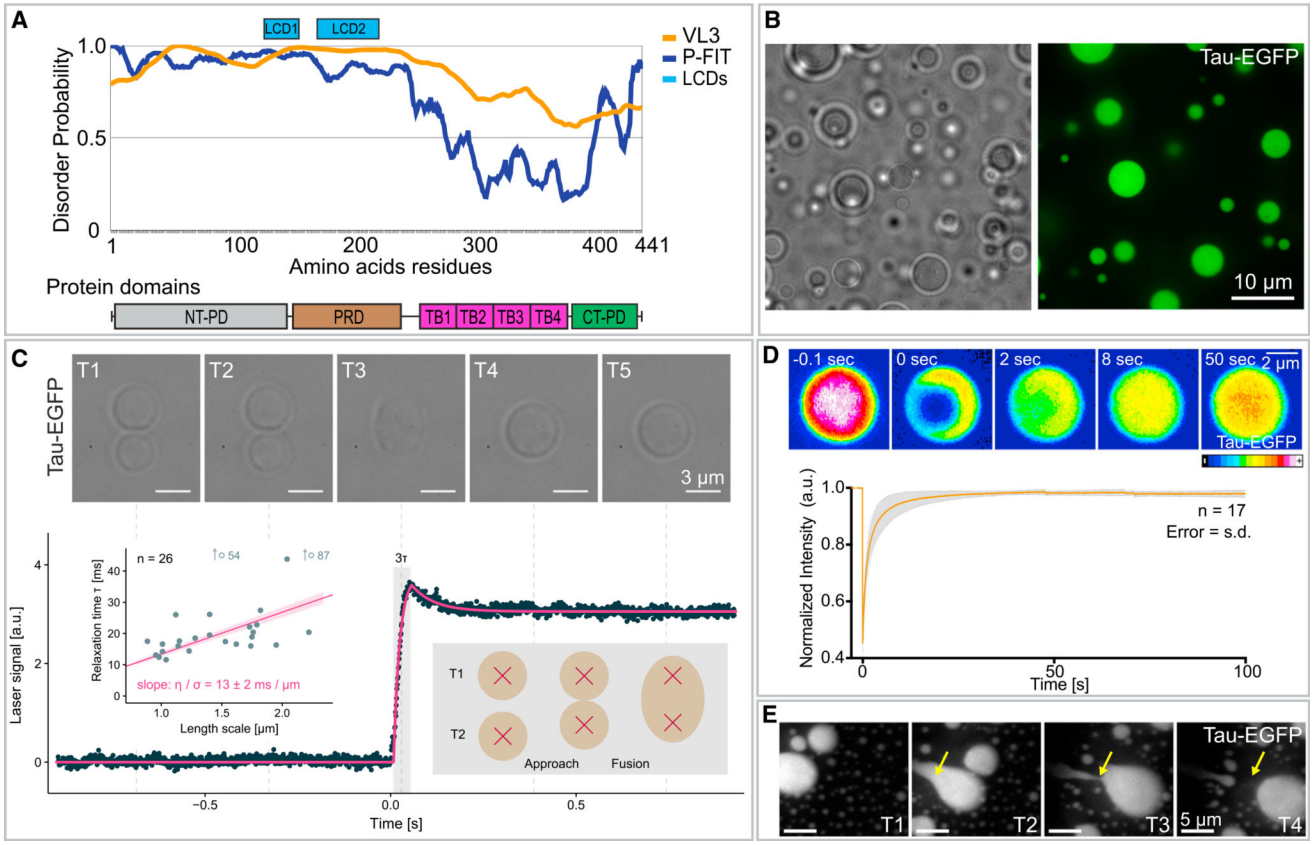

Figure 1. Tau Phase Separates into Liquid-like Drops

(A) Prediction of the degree of disorder along tau protein (htau441 isoform). PONDR-FIT (P-FIT) and VL3 algorithms are shown in blue and orange, respectively. A given region is considered disordered when the disorder probability is above 0.5. Low complexity domain (LCD)1 and LCD2 (pale blue rectangles) highlight regions of the protein with potential low complexity. Tau protein domains are shown below: NT-PD, N-terminal projection domain; PRD, proline-rich domain; TB1–TB4, tubulin binding repeats 1 to 4; CT-PD, C-terminal projection domain.

(B) Tau forms drops in vitro in the presence of 10% of crowding agent (dextran, T500). Bright-field and fluorescence microscopy images of tau-EGFP drops. See also Figure S2. Tau drops were formed with 25 µM tau-EGFP, 25 mM HEPES, 150 mM KCl, 1 mM DTT, and 10% dextran (pH 7.4) for all experiments in this figure. Recombinant tau was purified from insect cells. See SDS gel of purified proteins in Figure S1.

(C) Fusion of tau droplets using dual-trap optical tweezers. Top panel: time course of the fusion event (bright-field image) aligned to the laser signal (lower plot) recorded during fusion relaxation. See also Movie S1. The combined signal of the two traps is shown in the graph. Data were fit with two exponentials (magenta line). The τ constant (gray rectangle) for 26 fusion events of the fast, initial relaxation was plotted against the characteristic length of the droplet using the geometric radius (left inlet graph) to extract the ratio of dynamic viscosity to surface tension (slope). Data were fit with a robust linear fit (magenta line in inlet). Note the representation of 2 outliners by arrows, with their position indicated.

(D) Internal rearrangement of tau drops. Time course of fluorescence recovery after photo-bleaching (FRAP) after internal photo-bleaching of tau drops. LUT, Fiji 16 colors. See also Movie S2. Bottom panel: plot of the recovery in the photo-bleached area. Values shown are the mean ± SD, n = 17. Time 0 indicates the time for the photo-bleaching. Values were normalized to the first time point before photo-bleaching.
(E) Tau drop deformation by shear flow. Snapshots of Movie S3. Shear flow was applied from the top left to the bottom right of the image.

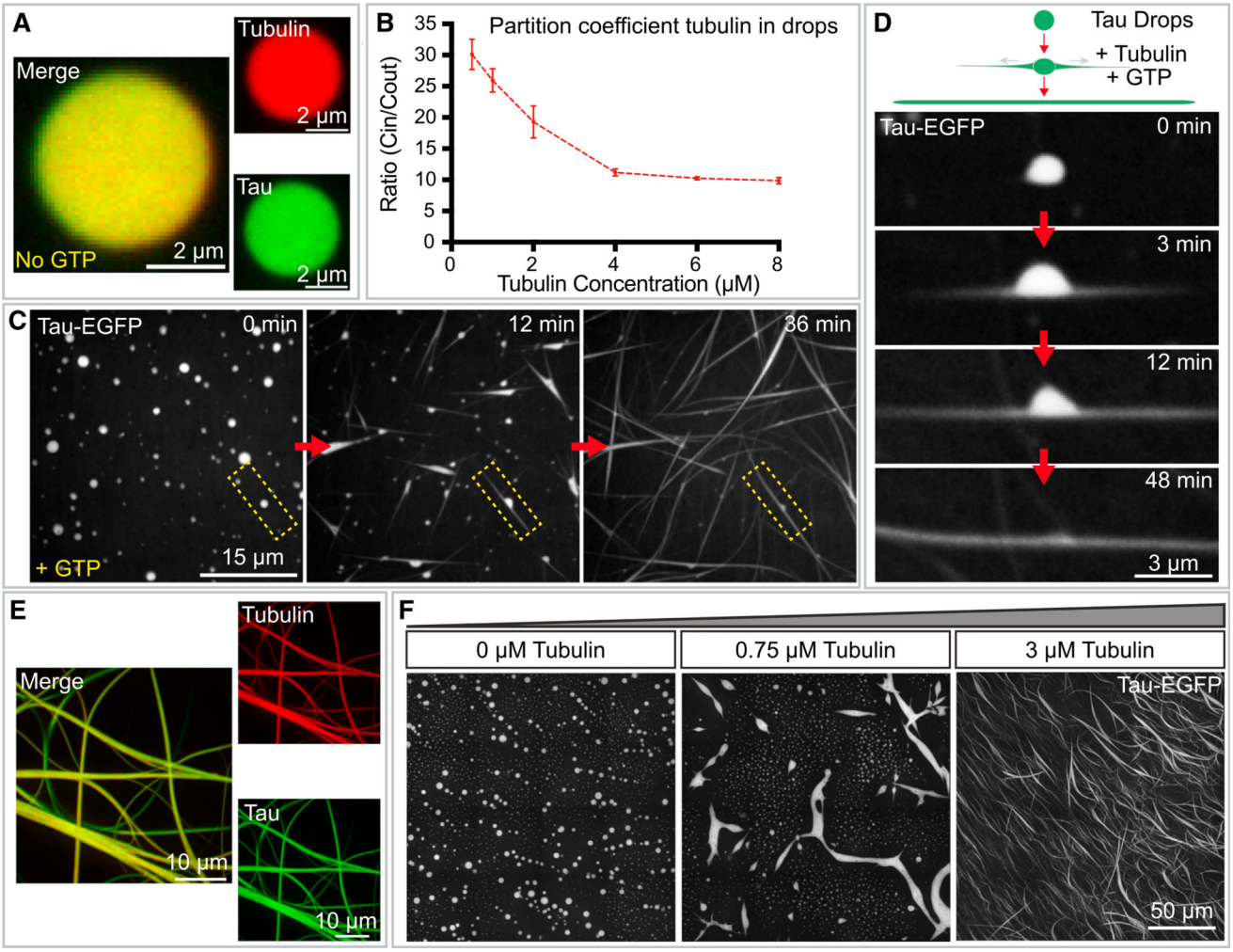

Figure 2. Tau Drops Concentrate Tubulin and Polymerize Tau-Encapsulated Microtubule Bundles

(A) Concentration of tubulin into tau drops. Merged and single-channel fluorescence microscopy images of tau drops (green) with incorporated tubulin dimers (red) 5min after mixing. An overall concentration of 5 μM rhodamine-labeled tubulin was added to tau drops. Tau drops were formed with 25 μM tau-EGFP in 13 BRB80 (pH 6.9) with 1 mM DTT and 10% dextran in all experiments with tubulin, if not otherwise mentioned.

(B) Tubulin partition coefficient quantified by the ratio of the mean intensity inside the drops to the mean intensity in the surrounding bulk media at different concentrations of overall tubulin (no GTP added). Values shown are the mean ± SD; n = 16 image stacks, 50 images per stack, mean of all drops in the stack. The concentration of tubulin in tau drops was above 10-fold in all concentrations of tubulin tested. See also Figure S3.

(C) Tau drop deformation by internal microtubule bundle polymerization. 5 μM rhodamine-tubulin were added to tau drops, together with 1 mM GTP. Immediately after the addition of tubulin, the drops deformed. See also Movie S4. All experiments in this paper were performed at room temperature (RT).

(D) Detail from the previous panel of a single drop deformation upon addition of tubulin and GTP. Drops deformed bidirectionally due to the polymerization of internal nucleated

microtubule bundles. Drops redistributed their volume along the growing microtubule bundles. See also Movie S5.

(E) Tau and tubulin co-localization in tau-encapsulated bundles formed from the deforming drops. Single-channel and merged maximum projection images are shown. The concentrations and conditions used are the same as in previous panels.

(F) Nucleation of tau-encapsulated bundles at low overall tubulin concentrations, 15 min after addition of tubulin. 0.75 μM of overall tubulin is sufficient to deform some drops by the internally nucleated microtubule bundles. Stitching of 16 maximum projection images is shown in each panel. Rhodamine-labeled tubulin was added at the indicated concentration to preformed tau drops.

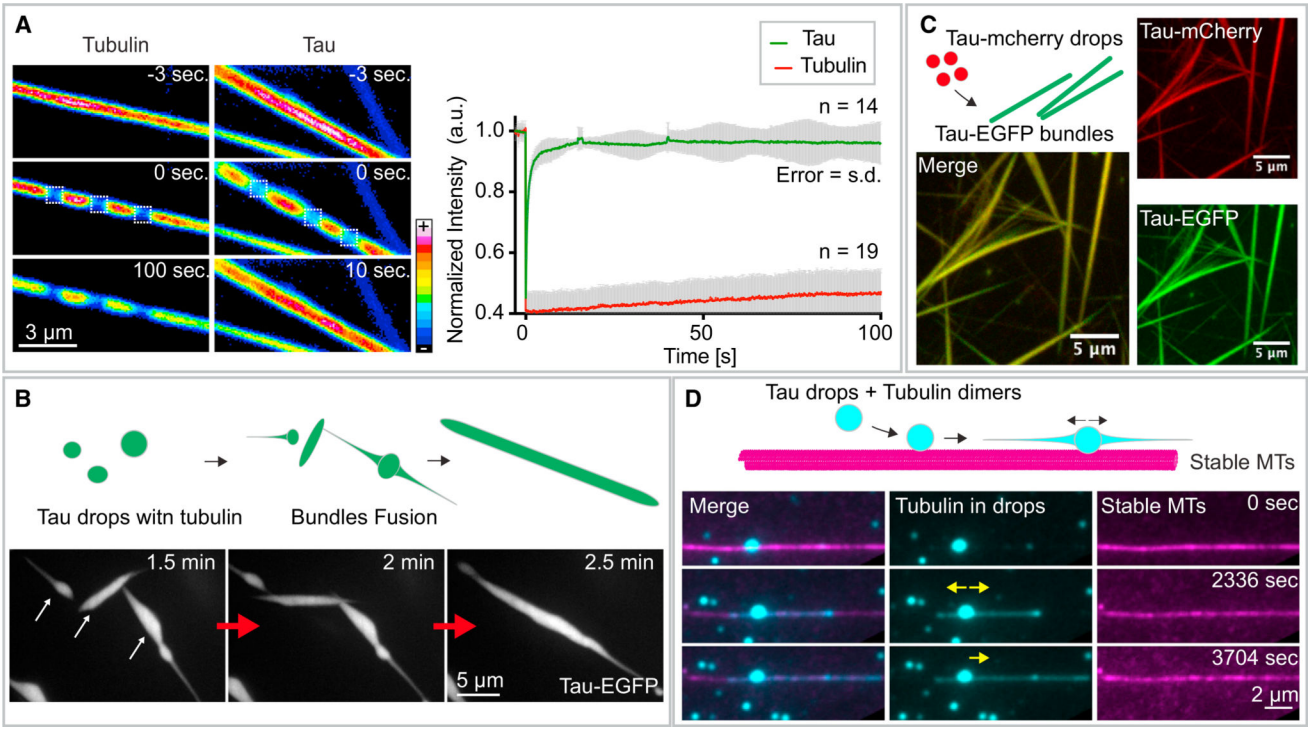

Figure 3. Tau in Tau-Encapsulated Microtubule Bundles Displays Liquid-like Properties

(A) Internal rearrangement of tubulin and tau in tau-encapsulated microtubule bundles. Left panel: time course of the recovery of the fluorescent signal after photo-bleaching for both tubulin (left row) and tau (right row) in bundles formed from tau drops. The recovery of 3 photo-bleached rectangular regions (dashed lines) is shown for each case. LUT, Fiji 16 colors. See also Movie S7. Right panel: quantification of the recovery for both tau (green) and tubulin (red) in bundles. Values shown are the mean ± SD; n = 14 (tau) and 19 (tubulin). Bundles were formed from tau drops with the protein concentrations and buffer conditions mentioned in previous figure.

(B) Tau-encapsulated microtubule bundle fusion. Time-course snapshots of the fusion of three bundles. See also Movie S8. Maximum projection fluorescence microscopy images of tau-EGFP are shown. Bundles were formed as mentioned earlier.

(C) Fusion of tau-mCherry drops to preformed tau-EGFP bundles. Bundles were formed from tau-EGFP drops as before but adding 5 µM of unlabeled tubulin, together with 1 mM GTP. Tau-mCherry drops were formed with 25 µM of tau-mCherry in same buffer conditions and added 1:2 to the bundles.

(D) Guided growth of microtubules polymerizing in drops along pre-existing microtubules. See also Movie S9. Tau drops were formed as in previous panels. 5 µM of Cy5-tubulin, together with 1 mM of GTP, were added to tau drops. Cy5-tubulin and GTP-loaded tau drops were flushed into a flow chamber containing immobilized and stable rhodamine-labeled microtubules. Microtubules growing in drops (cyan, Cy5-tubulin) grow in the direction of the adjacent pre-existing microtubule (magenta). Microtubules were double-stabilized using Taxol and GMP-CPP.

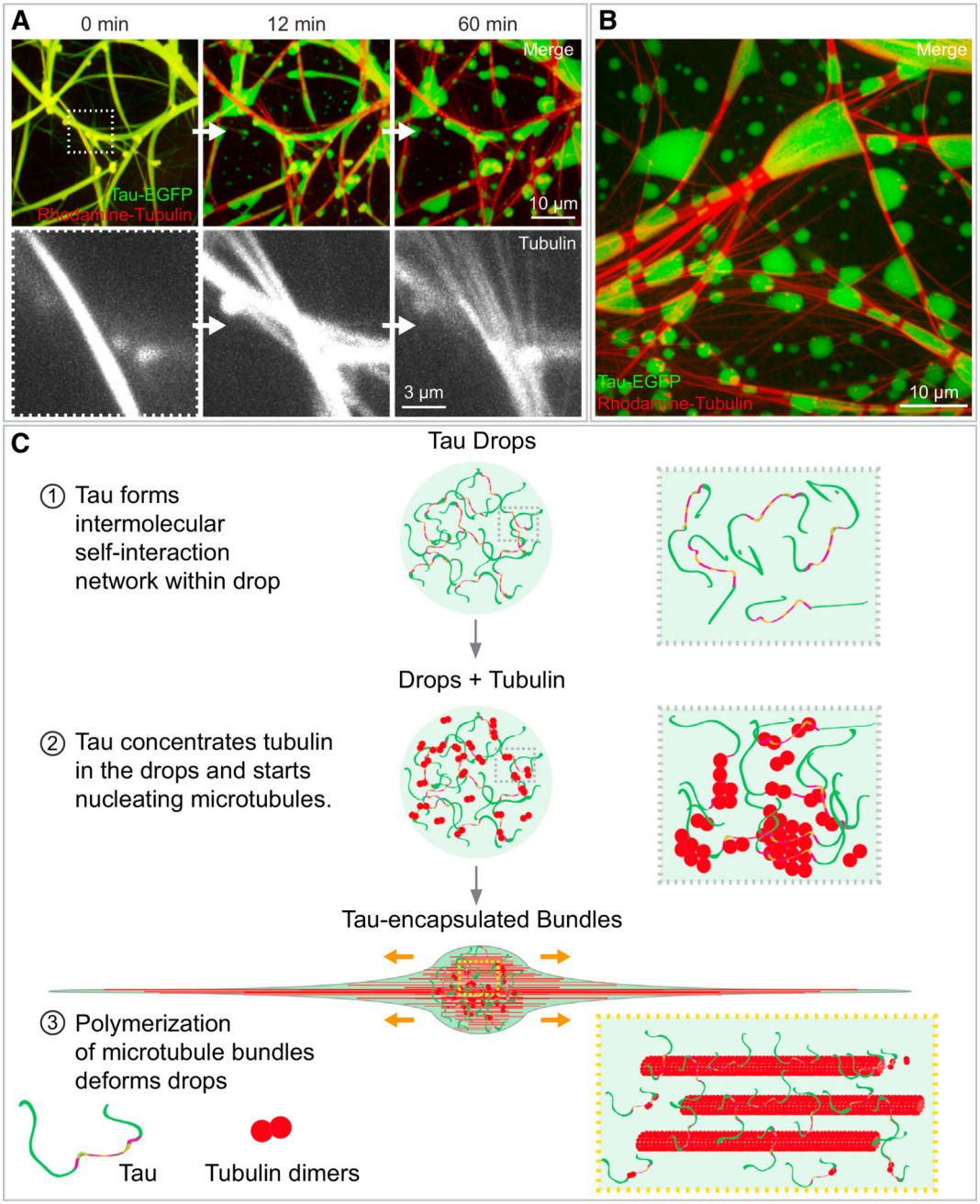

Figure 4. Tau Encapsulation Maintains Microtubule Bundles

(A) Heparin addition to tau-encapsulated bundles. Upper panels: time course of tau detachment from microtubule bundles, its reshaping back into drops, and the simultaneous debundling of microtubules upon addition of heparin. Tau-EGFP is shown in green, and rhodamine-tubulin is shown in red. See also Movie S10. Lower panel: detail of the microtubule debundling. 200 μg/mL of heparin were added to bundles formed with 5 μM rhodamine-tubulin and 1 mM GTP (protein concentration and buffer conditions as in previous figures). Maximum projection images are shown.

(B) Approximately 1 hr after heparin addition, tau is reshaped into both free and microtubule-attached drops. Conditions used are as in the previous panel.
(C) Proposed model for tau drop nucleation of microtubule bundles. (1) Tau's intrinsically disordered properties enable its phase separation in a crowded environment. (2) Tubulin dimers get concentrated inside tau drops, allowing microtubule nucleation inside tau drops. (3) Microtubule bundles grow within drops, deform it into a rod-like shape, and remain surrounded by liquid-like diffusible tau. Tau's simultaneous binding to multiple tubulin dimers by its four putative tubulin binding repeats, together with its intrinsically disordered arms, may be important for tubulin concentration and microtubule bundle nucleation and stabilization in drops.